Physics: Faculty Publications

Physics

1-1-2000

High Magnetic Field Corrections to Resistance Thermometers for Low Temperature Calorimetry

Nathanael Fortune
Smith College, nfortune@smith.edu

Gayle Gossett
Smith College

Lydia Peabody
Smith College

Katherine Lehe
Smith College

S. Uji
National Institute for Materials Science

See next page for additional authors

Recommended Citation

Fortune, Nathanael; Gossett, Gayle; Peabody, Lydia; Lehe, Katherine; Uji, S.; and Aoki, H., "High Magnetic Field Corrections to Resistance Thermometers for Low Temperature Calorimetry" (2000). Physics: Faculty Publications, Smith College, Northampton, MA.
https://scholarworks.smith.edu/phy_facpubs/79

Authors

Nathanael Fortune, Gayle Gossett, Lydia Peabody, Katherine Lehe, S. Uji, and H. Aoki

High magnetic field corrections to resistance thermometers for low temperature calorimetry

Nathanael Fortune, Gayle Gossett, Lydia Peabody, et al.
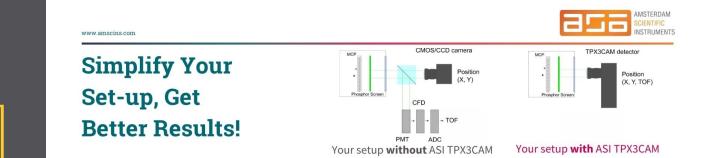
ARTICLES YOU MAY BE INTERESTED IN

High magnetic field corrections to resistance thermometers for low temperature calorimetry

Nathanael Fortune,[a] Gayle Gossett, Lydia Peabody, and Katherine Lehe
Department of Physics, Smith College, Northampton, Massachusetts 01063

S. Uji and H. Aoki
National Research Institute for Metals (NRIM), Tsukuba 305, Japan

We present a general analytical method of correcting for magnetic-field-induced changes in both the apparent temperature and the sensitivity of resistive thermometers at dilution refrigerator temperatures. With this method, we are able to reduce magnetic field induced errors in temperature to a level limited only by our ability to regulate the temperature in the absence of a magnetic field. We illustrate the application of our method to two resistive sensors in magnetic fields up to 18 T: a custom-made Au_xGe_{1-x} thin film sensor used in calorimetry and a commercially available ruthenium–oxide thick film resistor used in thermometry. © *2000 American Institute of Physics.* [S0034-6748(00)04810-3]

I. INTRODUCTION

Resistive thermometers often require corrections for magnetic-field-induced changes at low temperature. For measurements at fixed field, the most common method is to crosscalibrate a resistive thermal sensor in a series of magnetic fields against a second sensor in a field-free region at the same temperature. If the temperature dependence of the resistance can be fit to an analytic expression, then this expression can be differentiated to find two additional parameters essential to calorimetry: the dimensionless sensitivity η and the fractional change in temperature $\Delta T/T$, where

$$\eta \equiv -d \log R / d \log T \qquad (1)$$

and

$$\frac{\Delta T}{T} = -\frac{1}{\eta} \frac{\Delta R}{R} \qquad (2)$$

for $\Delta R/R \ll 1$, where $\Delta R/R$ is the measured fractional change in resistance.

For measurements in continuously varying magnetic fields, it is more common to measure the magnetoresistance of the sensor at a series of fixed temperatures, then fit it to an analytic expression with temperature dependent coefficients. This second method allows measurements of T as a continuous function of magnetic field B but often introduces large and systematic errors in η and $\Delta T/T$ due to the complex temperature dependence of the fitting coefficients. In contrast, the method we present here provides a simple and accurate means of correcting for field-induced errors in both T and η as a continuous function of magnetic field. We represent the temperature dependence of the resistance using a series of temperature-independent coefficients, and use mag-

netoresistance data at a series of fixed temperatures to find explicit expressions for the field dependence of these coefficients.

II. EXPERIMENT AND RESULTS

A. Sensor preparation and measurement

The Au_xGe_{1-x} sensor used in this study was a $Au_{0.18}Ge_{0.82}$ polycrystalline thin film specifically prepared for use as a calorimetric sensor. The polycrystalline film was formed from 50 Ge/Au bilayers sequentially sputtered at 40 °C onto a single crystal sapphire substrate with previously deposited Au/Cr contacts then postannealed at 265 °C.[1] The annealing process transforms the bilayers into a distribution of Au clusters confined to polycrystalline Ge grain boundaries through a process known as metal-assisted crystallization. The Au grain size and distribution and, consequentially, the low temperature sensitivity η depends on the annealing temperature; a 1 h anneal is necessary to eliminate changes in room temperature resistance due to further heat treatment at or below 265 °C.[1] A spark-bonding process[2] is used to attach electrical wires to the contacts without the use of solder or conductive epoxies.

The ruthenium–oxide thick film resistor used in this study is a commercially available 1 kΩ resistor (ALPS 102 A) designed for surface mounting on printed circuit boards.[3] Their small size, low cost, and ready availability have lead to interest in the use of ruthenium–oxide surface mount resistors as low temperature thermometers[4,5] even though their thick alumina substrates, protective epoxy coatings, and integrated solder pads with superconductive elements make them unsuitable for small sample calorimetry.

Once the Au_xGe_{1-x} and ruthenium–oxide films were prepared and wired, they were directly immersed into the mixing chamber of a top-loading ^3He–^4He dilution refrigerator equipped with an 18 T superconducting magnet. The films were crosscalibrated against two separate thermometers: a commercially calibrated Ge thermometer adjacent to

[a] Author to whom correspondence should be addressed; electronic mail: nfortune@science.smith.edu
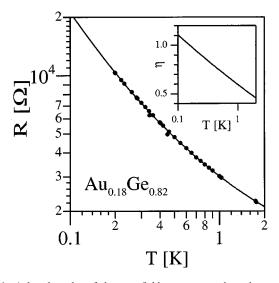
FIG. 1. A log–log plot of the zero-field temperature dependence of the resistance for a typical polycrystalline $Au_{0.18}Ge_{0.82}$ thin film after annealing at 265 °C. The solid line is an empirical fit to the $Au_{0.18}Ge_{0.82}$ data using a linear combination of Chebyshev polynomials. A log–linear graph of the temperature dependence of the dimensionless sensitivity η is included in the inset.
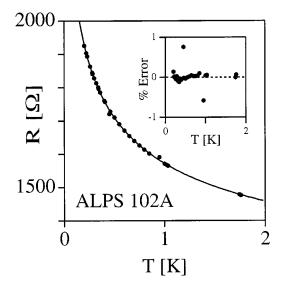

FIG. 2. Zero-field temperature dependence of the resistance for an ALPS 102 A ruthenium–oxide sensor. The solid line is an empirical fit to the data using a linear combination of Chebyshev polynomials. The inset is a plot of percent error in resistance vs temperature for the empirical fit, highlighting two outliers in the original data.

the films (in zero field) and a commercially calibrated ruthenium–oxide thermometer located in a field cancellation region above the films at the ^{3}H-rich^{3}He-poor phase boundary. A magnetic-field cancellation coil kept the magnetic field seen by the calibrated ruthenium–oxide thermometer to less than 180 G at 18 T (0.1%). Due to its large magnetoresistance, the Ge thermometer was not used during field sweeps, but was instead used to verify that the films were in thermal equilibrium with the ruthenium–oxide thermometer before each field sweep. The temperature of the ruthenium–oxide thermometer in the field cancellation region was regulated to within ±0.2% during each field sweep. In standard high field magnets without accompanying cancellation coils, a magnetic-field-independent glass[6,7] or Kapton-based[8] capacitor could be used for temperature control.

The temperature dependence of the resistance $R(T)$ in the absence of an applied magnetic field is plotted in Fig. 1 on a log–log scale between 0.1 and 2 K for a typical $Au_{0.18}Ge_{0.82}$ sensor annealed at 265 °C. The dimensionless sensitivity η is shown in an inset. The solid line is a third-order fit to $R(T)$ using a linear combination of Chebyshev polynomials, as described in Sec. III. The corresponding zero-field temperature dependence of the ALPS 102 A sensor is plotted in Fig. 2. As in Fig. 1, the solid line is an empirical fit to $R(T)$ using a linear combination of Chebyshev polynomials. The inset is a plot of percent error in resistance versus temperature for this fit. The fit and residual error highlight two outliers in the original data. The sensitivity η is low but nearly constant over the entire field and temperature range (η=0.125 ±0.005), in good agreement with an independent set of zero-field measurements below 1 K.[4]

To separate the magnetic field dependence of the resistance from this zero-field temperature dependence, we have re-expressed the resistance $R(T,B)$ in terms of the zero-field resistance $R(T,0)$ and the fractional magnetoresistance $f(T,B)$ where

$$f(T,B) = \frac{R(T,B) - R(T,0)}{R(T,0)}, \qquad (3)$$

following the approach of Naughton *et al.*[9] for carbon composition resistors. The field dependence of $f(T,B)$ for the $Au_{0.18}Ge_{0.82}$ sensor for a series of constant temperature field sweeps is presented in Fig. 3. The solid lines are fits to the data described in Sec. III. For clarity, only six of the 15 field sweeps between 0.1 and 1 K are shown, although all 15 were used to determine the magnetoresistance corrections.

The corresponding data and fits for the ALPS 102 A ruthenium–oxide sensor are presented in Fig. 4 for a few selected temperatures. Field sweeps at five different temperatures—0.207, 0.278 (not shown), 0.496, 0.596 (not
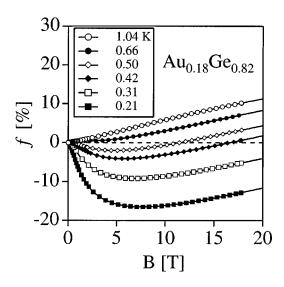

FIG. 3. Fractional magnetoresistance $f(T,B)$ of an $Au_{0.18}Ge_{0.82}$ sensor annealed at 265 °C for a series of constant temperature field sweeps from 0.1 to 1 K, where $f(T,B) = [R(T,B) - R(T,0)]/R(T,0)$. The solid lines are fits to the data using ratios of polynomials known as Padé approximants.
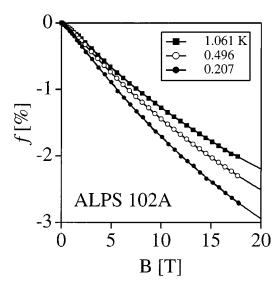
FIG. 4. Fractional magnetoresistance $f(T,B)$ of an ALPS 102 A ruthenium–oxide sensor for a series of constant temperature field sweeps. The solid lines are Padé fits to the data. Padé fits were also made to $f(T,B)$ data for 0.278 and 0.596 K (not shown).

shown), and 1.061 K—were used to determine the magnetoresistance corrections. The magnetoresistance is significantly smaller and monotonic, but because of the reduced sensitivity, the field induced percent error in apparent temperature (in the absence of field corrections) is still significant, ranging from 23% at 0.2 K to 20% at 1 K.

III. ANALYSIS

A. Basic method

In the absence of a magnetic field, we have previously shown that the temperature dependence of the resistance of Au_xGe_{1-x} thin films between 2 and 300 K can be fit to a linear combination of simple polynomials

$$\log R = \sum_{n=0}^{N} a_n [\log T]^n. \tag{4}$$

In this work, however, we find it preferable to re-express Eq. (4) in terms of a linear combination of type I Chebyshev polynomials $t_n(x) \equiv \cos(n \arccos x)$, where

$$
\begin{aligned}
t_0(x) &= 1, \\
t_1(x) &= x, \\
t_2(x) &= -1 + 2x^2, \\
t_3(x) &= -3x + 4x^3, \\
t_{n+1}(x) &= 2x t_n(x) - t_{n-1}(x),
\end{aligned}
\tag{5}
$$

where x is a function of $\log T$. The use of Chebyshev polynomials simplifies the magnetic field dependence of the series coefficients and improves the convergence of the fit at high fields. In addition, since $|t_n(x)| \leq 1$ for $-1 \leq x \leq 1$, the maximum contribution of each term in the series is readily evaluated provided $|x| \leq 1$.

The minimum and maximum temperatures of interest can be scaled to span the entire $-1 \leq x \leq 1$ range by use of the relation

$$x = \frac{(\log T - \log T_{\min}) - (\log T_{\max} - \log T)}{(\log T_{\max} - \log T_{\min})}. \tag{6}$$

For the temperature range $0.1 \leq T \leq 10$ K used in this study, Eq. (6) simplifies to $x = \log(T)$.

Using Eq. (6) to re-express $\log R$ in terms of $t_n(x)$, we have

$$\log R(T,B) = \sum_{n=0}^{N} c_n(B) t_n(x), \tag{7}$$

where c_n are magnetic field dependent fitting coefficients. Since the $c_n(B)$ are temperature independent and the $t_n(x)$ are field independent, temperature control reduces to the calculation of a magnetic-field-dependent resistance setpoint. Temperature measurement correspondingly reduces to the evaluation of Eq. (7) for a given measured R using standard root-search methods.

An additional advantage of Eq. (7) is the ease of calculation of two additional quantities needed for calorimetry: the logarithmic sensitivity η and the fractional change in temperature $\Delta T/T$. Since the derivative with respect to $\log T$ of a Chebyshev series in $\log T$ is itself a Chebyshev series in $\log T$, we can re-express the sensitivity η as

$$\eta = -\frac{d \log R}{d \log T} = -\frac{2}{(\log T_{\max} - \log T_{\min})} \sum_{n=0}^{N-1} d_n(B) t_n(x), \tag{8}$$

where the fitting coefficients d_n are related to the original coefficients c_n by the following recursion relations:[10]

$$
\begin{aligned}
d_0 &= \tfrac{1}{2}[d_2 + 2c_1] \quad (n=0), \\
d_n &= d_{n+2} + 2(n+1)c_{n+1} \quad (n=1,2,...N-1), \\
d_n &= 0 \quad (n \geq N).
\end{aligned}
\tag{9}
$$

We have found that with four terms—c_0, c_1, c_2, and c_3—we are able to fit the zero-field dependence of the resistance to within the accuracy of our measurements for both sensors. The corresponding coefficients d_n thus have values $d_0 = 3c_3 + c_1$, $d_1 = 4c_2$, and $d_2 = 6c_3$.

B. Data analysis

The first step in this analysis is to interpolate the fractional magnetoresistance $f(T_j, B)$ at constant temperature T_j at a series of magnetic field values B_k. For the Au_xGe_{1-x} sensor, we incremented B_k in steps of 0.2 T over the entire field range. For the ALPS 102 A ruthenium–oxide sensor, the errors in the measured resistance due to field-dependent sources exceed the fractional magnetoresistance below 1 T. We therefore increment the magnetic field B_k in larger steps of 2 T for this sensor. To avoid introducing nonphysical oscillations in the interpolated data and/or distortion of the data in the zero-field and high field limits, we have chosen to simultaneously interpolate and smooth the data by fitting it to a ratio of polynomial functions known as a Padé approximant[11]

$$f_{\text{data}}(B_{\text{data}}) \approx f_{\text{fit}}(B_{\text{data}}) = \frac{\sum_{p=1}^{P} \alpha_p [B_{\text{data}}]^p}{1 + \sum_{q=1}^{Q} \beta_q [B_{\text{data}}]^q}, \tag{10}$$

where the fitting coefficients α_p and β_q are determined by a nonlinear least squares fit to the data. Just as with curve
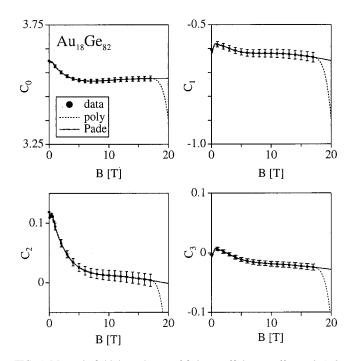
FIG. 5. Magnetic field dependences of fitting coefficients c_n (for $n=0, 1, 2, 3$) of $\log R = \Sigma c_n t_n(x)$, where $x = \log T$ and t_n is the nth order Chebyshev polynomial. Error bars correspond to ± 1 sd. The dashed lines represent fits to linear combinations of simple polynomials; the solid lines represent fits to a ratio of polynomials, known as a Padé approximant. These fits are used to evaluate c_n for arbitrary values of magnetic field B.

fitting to an ordinary polynomial, the appropriate number of terms needed to model the data must be chosen by the experimenter by trial and error. For the ruthenium–oxide and AuGe sensors presented here, we choose $P=Q=2$ and $P=Q=4$, respectively.

After using Eq. (10) to generate a set of resistance versus temperature values at constant B, we fit each data set to a series of Chebyshev polynomials with coefficients $c_n(B_k)$ by linear regression. The magnetic field dependence of the calculated coefficients c_0, c_1, c_2, and c_3 for the Au_xGe_{1-x} sensor is shown in Fig. 5. The error bars in c_n correspond to ± 1 sd in the determination of $c_n(B_k)$. To improve the clarity of the figures, error bars are only shown at a few representative values of B_k.

The dashed lines in Fig. 5 represent fits of c_n to linear combination of simple polynomials, while the solid lines represent fits to a Padé approximant. The weaknesses of using simple polynomials to approximate functions that vary in a complex but nonoscillatory manner is clear: the higher order terms needed to suppress nonphysical oscillations in the fitting function lead to strong divergences in the high and low field limits. In contrast, the Padé approximant $y_{n,k}$ provides an excellent, nondiverging fit to the data set, where

$$y_{n,k} \equiv c_n(B_k) - c_n(0) = \frac{\Sigma_{p=1}^p \kappa_{n,p}[B_k]^p}{1 + \Sigma_{q=1}^Q \gamma_{n,q}[B_\kappa]^q}. \qquad (11)$$

The coefficients $\kappa_{n,p}$ and $\gamma_{n,q}$ are both temperature and field independent. Once their values have been determined, no further recourse to the original magnetoresistance data is necessary.

To evaluate the accuracy of our fit of $\log R$ to $\log T$ for the Au_xGe_{1-x} sensor, we interpolated our calculated $\{B_k, c_n(B_k)\}$ data set to find $c_n(B)$ for each magnetic field value B and temperature T_j for which we had a *measured* value of R. We then used these interpolated values of c_n and the known temperature T_j in Eq. (7) to find R_{fit}, the expected value of R. Setting $\Delta R/R$ in Eq. (2) equal to the fractional deviation of R_{fit} from R_{data}, the fractional deviation of T_{fit} from T_{data} is given by

$$\frac{T_{fit} - T_{data}}{T_{data}} = \frac{1}{\eta(B)} \frac{[R_{fit}(B) - R_{data}(B)]}{R_{data}(B)}, \qquad (12)$$

where $\eta(B)$ is determined from Eq. (1) and $R_{fit}(B)$ is determined from Eq. (7).

The calculated fractional error in temperature $\Delta T/T_{data}$ is plotted versus temperature T_{data} for the Au_xGe_{1-x} sensor for representative values of magnetic field in Fig. 6. The solid symbols correspond to the calculated fractional error in temperature using our method; the hollow symbols correspond to the calculated fractional error in temperature using an alternative method described in Ref. 12. For our method, $\Delta T/T_{data} \leqslant 0.1\% - 0.3\%$, corresponding to the experimental limit of our ability to regulate the temperature in the absence of a magnetic field.

As a second test of the accuracy of our general expression for the resistance at arbitrary temperature and magnetic field, we calculated the fractional magnetoresistance $f(T,B)$ for the ALPS 102 A sensor at two temperatures not used in the calculation of the fitting coefficients: 0.420 and 0.769 K. The results are shown in Fig. 7. The solid lines are the original data. The symbols are *not* direct fits to the data using a Padé approximant; they are calculated values found using Eq. (7). The corresponding percent error in temperature $\Delta T/T$ versus magnetic field B after correcting for the magnetoresistance is $\leqslant 0.5\%$ for $B > 1$ T for both field sweeps. The slightly larger error in $\Delta T/T$ for this sensor compared to the Au_xGe_{1-x} sensor is due to a greater level of noise in the original data for the ruthenium–oxide sensor. For both sensors, the errors in $\Delta T/T$ are reduced to their zero-field level.

IV. COMPARISON WITH RELATED METHODS

In Sec. III, we presented a three step method that results in expressions for R, η, and $\Delta T/T$ in terms of B and T. In this section, we compare our method to three alternatives: a direct, *in situ* crosscalibration at a series of discrete field values and two previously published semiempirical models.

When making calorimetric measurements as a function of temperature at a series of discrete field values, it may be possible to calibrate the resistive sensor as a function of temperature in a magnetic field against a thermometer placed in a field-free region held at the same temperature. After calibration, the sensor can be moved to a magnet without a cancellation coil if the same magnitude magnetic field is reapplied. In many experiments, however, a field free region at the same temperature is not available and the appropriate values of magnetic field are not known in advance. Even if a field cancellation region is available, an analytic expression for arbitrary B may still be desirable, since it offers the pros-
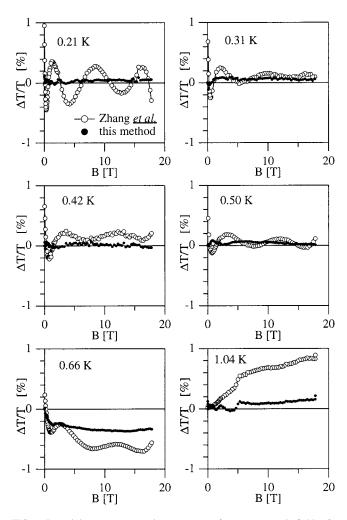
FIG. 6. Remaining percent error in temperature $\Delta T/T$ vs magnetic field B for selected temperature sweeps after correcting for the magnetoresistance of the $Au_{0.18}Ge_{0.82}$ sensor. The solid symbols correspond to the remaining fractional error in temperature after using the correction method presented in this article; the hollow symbols correspond to the fractional error in temperature after using the alternative correction method of Ref. 12. Our method reduces the magnetoresistance-induced errors in $\Delta T/T$ to a level corresponding to the experimental limit of our ability to regulate the temperature during field sweeps.
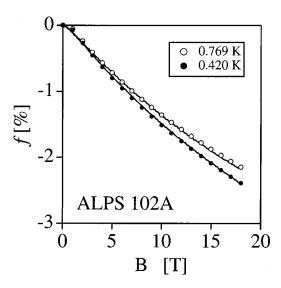

FIG. 7. Comparison of measured and calculated fractional magnetoresistance $f(T,B)$ for an ALPS 102 A ruthenium–oxide sensor for field sweeps at two temperatures: 0.420 and 0.769 K. The solid lines are the original data. The symbols are *not* direct fits to the data using a Padé approximant; they are calculated values found using our general expression for the resistance at arbitrary temperature T and magnetic field B: $\log R(T,B)=\Sigma c_n(B)t_n(\log T)$, where t_n is the nth order Chebyshev polynomial and $c_n(B)$ is the corresponding nth order magnetic-field dependent Chebyshev coefficient.

$$R(T,B)=\sum_{n,m} d_{m,n}R(T,0)^m B^n. \tag{13}$$

The coefficients $d_{m,n}$ are determined by first fitting the resistance to a simple polynomial in B given by

$$R_i(B)=\sum_n b_{n,i}B^n, \tag{14}$$

where the coefficients $b_{n,i}$ are implicitly temperature dependent due to their dependence on the zero field resistance $R(T,0)$ at temperature T_i:

$$b_{n,k}=\sum_m d_{n,n}R(T_i,0)^m. \tag{15}$$

To determine T from R at any B, the corresponding zero field resistance $R(T,0)$ is first found from $R(T,B)$ using Eq. (13) and standard root-search methods. Given $R(T,0)$, the temperature T can then be found from the zero field calibration of R vs T. This alternative method is reported to reduce field-induced errors in $\Delta T/T$ to a few percent for both a ruthenium–oxide sensor at dilution refrigerator temperatures and a commercial zirconium–oxynitride sensor at liquid ^{4}He temperatures in fields up to 17 and 31 T, respectively.[12]

When we apply the method of Ref. 12 to our own Au_xGe_{1-x} sensor data, we find that once the number of fitting coefficients has been optimized, the field induced errors are typically reduced to between 0.5% and 1%. As can be seen in Fig. 6, the principal drawback to the method of Ref. 12 is the oscillatory and occasionally diverging nature of the error in $\Delta T/T$. We attribute the oscillations in $\Delta T/T$ to the intrinsically oscillatory dependence of the fitting coefficients $b_{n,i}$ on $R(T,0)$ in Eq. (15) and to nonmonotonic systematic errors in $\Delta T/T$ introduced by the need for two separate root-finding steps for $T(R)$ and $T(R+\Delta R)$.

pect of reducing the number of fields at which a time consuming direct calibration is required.

A second alternative to our approach is to directly fit the magnetoresistance to a physical model with temperature-dependent coefficients. In one of the more successful models for carbon-composition resistors,[9] the fractional magnetoresistance $f(T,B)$ is assumed to be due to a competition between two terms: one positive and one negative. In this work, we have tried to fit our $f(T,B)$ data for the Au_xGe_{1-x} sensor to this model but were met with only limited success. In no case was our agreement in $\Delta T/T$ better than 10%. Direct calculations of the sensitivity η proved to be impossible due to the complex dependence of the fractional magnetoresistance on its temperature dependent coefficients and the wide range of possible expressions for the temperature dependence of each coefficient.

In the last of the three methods we considered,[12] the resistance $R(T,B)$ is expressed in terms of powers of B and $R(T,0)$

The improved accuracy of our method is due in part to: (1) the use of Chebychev polynomials, which recast the relation between $\log R$ and $\log T$ in a form that does not require numerical differentiation to find η and (2) the use of Pade approximants, which suppress artificial oscillations and divergences in the calculated field dependence of R, η, and $\Delta T/T$. Since magnetic-field induced quantum oscillations in specific heat and the magnetothermal effect[13,14] are typically on the order of 0.1%–1%, the improved suppression of field-dependent errors beyond the 1%–10% level of accuracy offered by previous methods is a significant advantage.

ACKNOWLEDGMENTS

[1] N. A. Fortune, M. J. Graf, and K. Murata, Rev. Sci. Instrum. **69**, 133 (1998).

[2] N. A. Fortune (unpublished).

[3] ALPS 102 A, ALPS Electric Inc. 3553 N. First St., San Jose, CA 95134.

[4] A. Briggs, Cryogenics **31**, 932 (1991).

[5] R. G. Goodrich, D. Hall, E. Palm, and T. Murphy, Cryogenics **38**, 221 (1998).

[6] P. Strehlow, Cryogenics **34**, 421 (1994).

[7] F. C. Penning, M. M. Major, S. A. J. Wiegers, H. Van Kempen, and J. C. Mann, Rev. Sci. Instrum. **67**, 2602 (1996).

[8] T. P. Murphy, E. C. Palm, L. Peabody, and S. W. Tozer (unpublished).

[9] M. J. Naughton, S. Dickinson, R. C. Samaratunga, J. S. Brooks, and K. P. Martin, Rev. Sci. Instrum. **54**, 1529 (1983).

[10] E. T. Goodwin, *Modern Computing Methods,* 2nd ed. (National Physical Laboratory, London, 1961), p. 79.

[11] N. A. Gershenfeld, *The Nature of Mathematical Modeling* (Cambridge University Press, Cambridge, UK, 1999), p. 140.

[12] B. Zhang, J. S. Brooks, J. A. A. J. Perenboom, S.-Y. Han, and J. S. Qualls, Rev. Sci. Instrum. **70**, 2026 (1999).

[13] P. F. Sullivan and G. Seidel, Phys. Rev. **173**, 679 (1968).

[14] N. A. Fortune, M. A. Eblen, S. Uji, H. Aoki, J. Yamada, S. Tanaka, S. Maki, S. Nakatsuji, and H. Anzai, Synth. Met. **103**, 2078 (1999).